



Contents lists available at ScienceDirect

Journal of Biomechanics

journal homepage: [www.elsevier.com/locate/jbiomech](http://www.elsevier.com/locate/jbiomech)  
[www.JBiomech.com](http://www.JBiomech.com)

# An evolutionary model of osteoarthritis including articular cartilage damage, and bone remodeling in a computational study

Michael E. Stender<sup>a</sup>, R. Dana Carpenter<sup>a</sup>, Richard A. Regueiro<sup>b</sup>, Virginia L. Ferguson<sup>a,\*</sup>

<sup>a</sup> Department of Mechanical Engineering, University of Colorado, Boulder, CO 80309, United States

<sup>b</sup> Department of Civil, Environmental, and Architectural Engineering, University of Colorado Boulder, CO 80309, United States

## ARTICLE INFO

### Article history:

Accepted 16 September 2016

### Keywords:

Bone remodeling  
Articular cartilage damage  
Finite element analysis  
Osteoarthritis  
Cross talk

## ABSTRACT

With osteoarthritis, a complex set of progressive chemical, biological, and mechanical changes occur in both cartilage and bone. The aim of this study is to develop a high-fidelity computational model of the complete bone–cartilage unit to study the evolution of osteoarthritis-induced articular cartilage (AC) damage and remodeling of subchondral cortical bone (SCB) and subchondral trabecular bone (STB). A finite element model of spherical indentation was developed with a depth-dependent anisotropic model of degenerating articular cartilage, a calcified cartilage (CC) zone, and SCB and STB remodeling regions. Calcified tissue (CC, SCB, and STB) and AC material regions were integrated to form an evolutionary bone–cartilage unit model. Results indicate that with indentation loading, articular cartilage damage occurs at the articular surface. Furthermore, bone remodeling was predicted to occur with a net stiffening of the subchondral bone plate. Changes in indentation force were minimal ( $< 2\%$ ) between initial and final peak indentation loading. However, additional degradation and wear of AC and/or alterations in loading may have more pronounced effects on the mechanical response of the bone–cartilage unit. Bone remodeling and articular cartilage damage predictions are consistent with experimental observations that cartilage damage begins at the articular surface and subchondral bone experiences a thickening (*i.e.*, stiffening) response with osteoarthritis. Our results provide insight into the early-term initiation behavior of osteoarthritis; the potential consequences of evolutions in AC, SCB, and STB with disease progression; and may guide future experimental and computational studies to elucidate mechanisms of osteoarthritis progression.

© 2016 Elsevier Ltd. All rights reserved.

## 1. Introduction

The synovial joint is exquisitely designed to transfer stresses and strains through the highly dissimilar tissues of bone and cartilage. However, degeneration and subsequent remodeling of any single osteochondral tissue, such as observed in osteoarthritis—the primary pathology in synovial joints, disrupts normal stress and strain transfer. Recent studies demonstrate the importance of considering the complete bone–cartilage unit (BCU), as opposed to any single osteochondral tissue when studying osteoarthritis initiation and progression of (Goldring and Goldring, 2010; Lories and Luyten, 2010; Burr and Gallant, 2012). In addition to articular cartilage (AC) and calcified tissues, synovial joints contain a variety of additional tissues including synovium, bursae, menisci, ligaments, tendons, and articular fat pads. For simplicity, in this work only AC, calcified

cartilage (CC), subchondral cortical bone (SCB), and subchondral trabecular bone (STB) are considered. Remodeling of the calcified tissues that leads to either softening or stiffening is integral to osteoarthritis pathogenesis (Grynblas et al., 1991; Bobinac et al., 2003; Burr, 2004; Burr and Gallant, 2012). However, the etiology of degenerative changes in OA remains unclear. Osteoarthritis symptoms may occur simultaneously in calcified tissues and AC (Lories and Luyten, 2010), or for non-traumatic osteoarthritis changes in bone may antedate AC degradation (Goldring and Goldring, 2010). The contemporary consensus is that osteoarthritis is a degeneration of the complete BCU rather than an independent degeneration of any single tissue (Brandt et al., 2006; Burr and Gallant, 2012). Yet, no consensus exists on exactly how osteoarthritis progresses within the BCU.

Physical changes observed in osteoarthritis suggest an inter-relationship between AC degeneration and evolutionary change of calcified BCU tissues. For example, osteoarthritis in mice (Botter et al., 2008) and canines (Sniekers et al., 2008) demonstrates similar patterns of initially thinning and subsequently thickening

\* Correspondence to: Department of Mechanical Engineering University of Colorado 427 UCB Boulder, CO 80309, USA. Fax: +1 303 492 7698.

E-mail address: [virginia.ferguson@colorado.edu](mailto:virginia.ferguson@colorado.edu) (V.L. Ferguson).

SCB with associated temporal changes in subchondral plate porosity (Sniekers et al., 2008; Botter et al., 2011). Correspondingly, increased bone porosity, a more textured surface, and increased osteoclast resorption pits indicating elevated remodeling activity were observed in osteoarthritic human femoral heads (Li et al., 1999). The experimentally observed thickening of calcified tissues within the subchondral bone plate results in stiffening of the joint structure (Burr, 2004) that modifies strain distributions, and porosity alterations affect fluid flow patterns (Hwang et al., 2008; Pan et al., 2009; Suri and Walsh, 2012) across cartilage and bone.

Osteoarthritic AC experiences degenerative chemical, mechanical, and structural changes (Brocklehurst et al., 1984; Grushko et al., 1989; Temple-Wong et al., 2009). AC, degeneration typically starts at the superficial zone (SZ) and progresses deeper into the middle zone (MZ) and the deep zone (DZ) (Pritzker et al., 2006; Thambyah and Broom, 2007; Saarakkala et al., 2010). Diminished tensile strength, likely as a result of collagen fibril failure, as well as an increase in water volume fraction, is observed in osteoarthritic AC (Temple et al., 2007; Temple-Wong et al., 2009). Furthermore in osteoarthritic AC, compressive and shear moduli decrease (Setton et al., 1999) likely due to a decrease in glycosaminoglycan molecule concentration (Maroudas and Venn, 1977; Venn and Maroudas, 1977; Brocklehurst et al., 1984; Temple-Wong et al., 2009).

The aim of the present study is to integrate appropriate computational modeling techniques to better understand the changes that occur in osteoarthritis. We hypothesize that key relationships (e.g., mechanical cross-talk) between articular cartilage degeneration and SCB stiffening are related and can be elucidated by combining evolutionary material models with differential material regions that represent the complete BCU. In this study, we examine the independent and combined effects of AC damage and bone remodeling within a model of the complete BCU. This model provides a foundation to evaluate scenarios that are difficult, if not impossible, to perform experimentally. Future refinement to include factors such as interstitial fluid flow and/or cellular signaling will provide further insight into how osteoarthritis initiates and progresses.

## 2. Methods and materials

A finite element model of the BCU was implemented in Abaqus (v6.13). The user material subroutine was used to model the material behaviors of AC, SCB, and STB. To model SCB and STB, a previously established bone remodeling algorithm (Beaupré et al., 1990a, 1990b) was used. An anisotropic damage model of AC (Stender et al., 2012, 2015) was used to model the superficial, middle, and deep zones of AC. Brief descriptions of the material models are provided below.

### 2.1. Bone remodeling

The algorithm proposed by Beaupré et al. (1990a, 1990b), is used here for SCB and STB. SCB and STB are modeled as linearly elastic, isotropic materials, where elastic moduli evolve based on applied loading. The daily stress stimulus,  $\Psi_b$  is introduced to quantify the cumulative applied loading at the continuum level as follows.

$$\Psi_b = \left( \sum n_i \sigma_i^m \right)^{\frac{1}{m}} \quad (1)$$

where  $n_i$  is the number of load cycles of load type  $i$ ,  $m = 4$  is the stress exponent that weights the importance of stress magnitude and load cycles, and  $\sigma_i$  is a continuum level stress of load type  $i$  defined as

$$\sigma_i = (2EU)^{\frac{1}{2}} \quad (2)$$

where  $E$  is continuum elastic modulus and  $U$  is the continuum strain energy density. The calculated value of  $\Psi_b$  for a given load type  $i$  and number of cycles is used to determine the remodeling rate,  $\dot{r}$  from Carpenter and Carter (2008) (Fig. 1).

The remodeling rate,  $\dot{r}$ , is the apposition-resorption rate ( $\mu\text{m}/\text{day}$ ).  $\Psi_b$  is the daily tissue level stress stimulus as determined by cycles and loading.  $\psi_{as} = 50$  MPa is the attractor state stress value where no net remodeling or resorption occurs. The bone remodeling rate,  $\dot{r}$ , is converted to a density evolution via the following relationship

$$\rho = \dot{r} S_v \rho_i \Delta t + \rho_0 \quad (3)$$

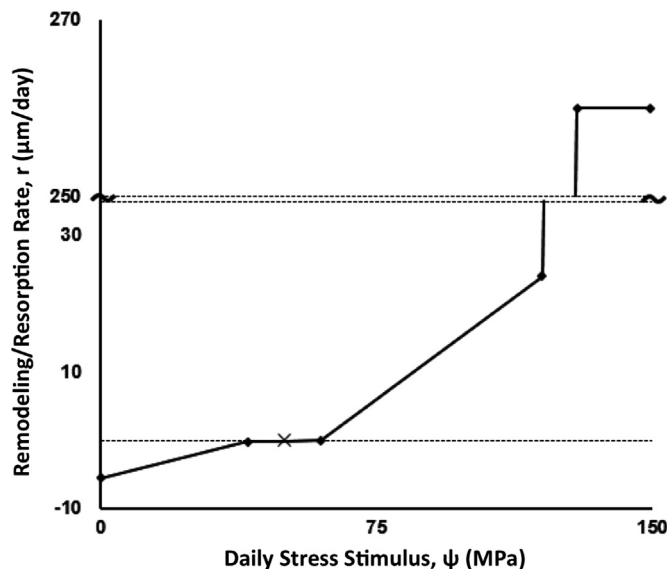


**Fig. 1.** The Bone remodeling rate,  $\dot{r}$ , as a function of daily stress stimulus,  $\Psi$ , based on experimental results as used in Carpenter and Carter (2008), showing that bone remodeling is decreased/suppressed for low  $\Psi$  values and increased/promoted with greater  $\Psi$  values. The attractor state corresponds to a loading state where there is no net change in bone volume (i.e. resorption rate is equal to the deposition rate).

where  $S_v$  is the bone surface area per unit tissue volume ( $4 \mu\text{m}^{-1}$ ),  $\rho_i$  is the true density of bone (i.e. the density of fully mineralized tissue), and  $\rho_0$  is the initial density of bone from the previous step that is initially set to  $1.5818 \frac{\text{g}}{\text{cm}^3}$  for SCB and  $0.6414 \frac{\text{g}}{\text{cm}^3}$  for STB (Beaupré et al., 1990b). The elastic modulus of SCB and STB is calculated as (Eser et al., 2013).

$$E = 3790\rho^3 \quad (4)$$

The elastic modulus (Eq. (4)) is implemented into a linear elastic constitutive material model and updated at each time step throughout the solution.

### 2.2. Articular cartilage damage model

A previously established model (Stender et al., 2015) of anisotropic AC damage was used. Briefly, strain-based damage is assumed to develop in collagen fibrils or glycosaminoglycan molecules. Collagen fibrils are assumed to behave with an elastic-brittle damage behavior in tension and to provide no resistance in compression. Pure compression is supported through contributions from glycosaminoglycan and ground substance matrix constituents. The second Piola-Kirchhoff stress tensor for the collagen fibril constituent,  $\mathbf{S}^{\text{COL}}$  is shown below

$$\mathbf{S}^{\text{COL}} = \frac{1}{4\pi} \int_{\phi=0}^{2\pi} \int_{\theta=0}^{\pi} H(E_N) \phi_N^f E^f E_N \left[ 1 - d_N^f \right] [\mathbf{N} \otimes \mathbf{N}] \sin \theta d\theta d\phi \quad (5)$$

where  $E_N$  is the Lagrangian fibril strain in direction  $N$ ,  $H$  is the Heaviside step function operator,  $\phi_N^f$  is the fibril tissue volume fraction in direction  $N$ ,  $E^f$  is the fibril elastic modulus (MPa),  $d_N^f$  is the fibril damage parameter which is zero for undamaged fibrils and 1 for damaged fibrils, and  $\theta$  and  $\phi$  are angles within a spherical coordinate system to determine the unit direction vector  $\mathbf{N} = \cos(\theta) \sin(\phi) \hat{\mathbf{i}} + \sin(\theta) \sin(\phi) \hat{\mathbf{j}} + \cos(\phi) \hat{\mathbf{k}}$ . Note that  $\mathbf{S}^{\text{COL}}$  is a volume integral in 3 dimensional space over a unit sphere, where  $r = 1$  is used to reduce the order of integration. The unit sphere is discretized into  $N$  equally dispersed pyramidal volume elements, each with a corresponding fibril volume fraction,  $\phi_N^f$  (Shirazi et al., 2011).

Glycosaminoglycan molecules are assumed to incur damage as a result of volumetric compression. Glycosaminoglycan damage is enforced as a reduction in molecule density that is hypothesized to result from a leeching and/or cleaving of glycosaminoglycan molecules from AC (Rolauffs et al., 2010; Stender et al., 2015). Presently, enzymatic degradation and other biochemical alterations in GAG concentration are not independently considered. The Second Piola-Kirchhoff stress tensor for the glycosaminoglycan constituent,  $\mathbf{S}^{\text{GAG}}$  is

$$\mathbf{S}^{\text{GAG}} = J \mathbf{F}^{-1} \left( -\alpha_1 \left( \frac{\rho_0^{\text{GAG}}}{J} \right)^{\alpha_2} \left\{ 1 - d_{\text{max}}^{\text{GAG}} \left[ e^{\left( \frac{-\theta}{\eta} \right)} - e^{\left( \frac{-\eta}{\theta} \right)} \right] \right\} \right) \mathbf{F}^{-T} \quad (6)$$

where  $J = \det \mathbf{F}$  is the determinant of the deformation gradient tensor,  $\mathbf{F}$ ,  $\alpha_1$  and  $\alpha_2$  are glycosaminoglycan constituent material constants from Stender et al. (2012),  $\rho_0^{\text{GAG}}$  is the molecule density in the reference configuration (mg/ml),  $d_{\text{max}}^{\text{GAG}}$  is a

Download English Version:

<https://daneshyari.com/en/article/5032561>

Download Persian Version:

<https://daneshyari.com/article/5032561>

[Daneshyari.com](https://daneshyari.com)